Hydrological effects of live poles on transient seepage in an unsaturated soil slope

Ng, Charles W. W.; Leung, Anthony K.; Yu, Ruiwang; Kamchoom, Viroon

Published in:
Journal of Geotechnical and Geoenvironmental Engineering

DOI:
10.1061/%28ASCE%29GT.1943-5606.0001616

Publication date:
2016

Document Version
Peer reviewed version

Hydrological effects of live poles on transient seepage in an unsaturated soil slope: A centrifuge and numerical study

Charles W. W. Ng[1], Anthony K. Leung*[2], Ruiwang Yu[1], Viroon Kamchoom[1]

Name: Dr Charles, Wang Wai NG
Affiliation: Chair Professor, Department of Civil and Environmental Engineering, Hong Kong University of Science and Technology
Address: Department of Civil and Environmental Engineering, Hong Kong University of Science and Technology, Clear Water Bay, Kowloon, Hong Kong

Name: Dr Anthony, Kwan LEUNG* (Corresponding author)
Affiliation: Lecturer in Civil Engineering, School of Science and Technology, University of Dundee
Address: Fulton Building, School of Science and Technology, University of Dundee, Nethergate, UK, DD1 4HN
E-mail: a.leung@dundee.ac.uk, **Telephone**: +44(0)1382 384390, **Fax**: +44(0)1382 384389

Name: Mr Ruiwang, YU
Affiliation: Department of Civil and Environmental Engineering, Hong Kong University of Science and Technology
Address: Department of Civil and Environmental Engineering, Hong Kong University of Science and Technology, Clear Water Bay, Kowloon, Hong Kong

Name: Dr Viroon, KAMCHOOM
Affiliation: Department of Civil and Environmental Engineering, Hong Kong University of Science and Technology
Address: Department of Civil and Environmental Engineering, Hong Kong University of Science and Technology, Clear Water Bay, Kowloon, Hong Kong

ABSTRACT:
Live poles have been used to stabilise shallow slopes. Most of the existing work has focused on pole reinforcement. The effects of pole transpiration on slope stability are unclear. This study aims to investigate the effects of pole transpiration on rainfall-induced slope hydrology through centrifuge model tests. A novel live pole modelling technique using real branch cuttings was adopted to simulate the hydrological effects of the transpiration-induced suction in the centrifuge. Suction responses during rainfall were recorded and back-analysed by seepage analysis. Higher suction was preserved after rainfall when pole transpiration induced higher suction before rainfall. This is because inducing higher suction would lower the soil water storage capacity and hydraulic conductivity. After a rainfall event with a return period of 20 years, up to 10 kPa of suction was preserved in the pole-supported slope to provide stabilisation effects.
KEYWORDS: Slope stability, live poles, transpiration, suction, centrifuge modelling

Introduction

Slope bioengineering using vegetation has been recognised as an environmentally-friendly way of stabilising shallow slopes. The method makes use of the so-called "live poles" (branch cuttings) to stabilise the top 1 to 2 m of a shallow slope (Steele et al. 2004; Wu et al. 2014). These live poles act as a structural element to provide mechanical reinforcement (Kamchoom et al. 2014). Later on when roots develop, transpiration becomes significant which induces soil suction. An increase in suction would increase the soil shear strength and reduce the hydraulic conductivity (Ng and Leung 2012). The field monitoring work conducted by Steele et al. (2004) has shown that soil slopes reinforced by live poles have greater stability than bare slopes. They found that the suction induced in pole-supported slopes at depth (up to 1.5 m) was 20% – 60% higher than that in bare slopes, depending on plant species and seasons. The hydrological effects of poles were prominent in hot and dry summer months, but were less significant in wet autumn. Although no slope failure was reported in Steele et al. (2004) and Wu et al. (2014), the underlying mechanisms of soil-pole interaction remained unclear, especially under the effects of live pole transpiration.

Centrifuge modelling is increasingly used to study the mechanical root reinforcement in scale model slopes (Sonnenberg et al. 2010, 2012). The principle of this technique is to test a $1/N^{th}$ scale model of real soil and to recreate stress conditions equivalent to those in a much larger prototype system. As the soil behaviour chiefly depends upon the confining pressure, stress levels must be recreated correctly to obtain an accurate soil response. This is achieved by increasing the centrifugal acceleration applied to the model to N times the Earth's gravitational acceleration (i.e., **g** level). In this way, the dimensions of a prototype system could be scaled down by N times. The seepage velocity of a prototype system could be increased by N times, while the seepage time could be decreased by N^2 times. In centrifuge model tests, the properties and boundary conditions of materials can be much better

controlled than in field experiments. Although extensive research has taken advantage of centrifuge modelling to provide useful information about mechanical root reinforcement, the effects of pole root-water uptake and hence the induced change in suction on slope stability have received little attention and are still unclear.

It has long been argued that during rainfall, the high relative humidity conditions would suppress plant transpiration. Hence, negligible soil suction would be preserved after rainfall (Sidle et al. 1985). This argument, however, ignores the antecedent drying effects of plant transpiration, which could affect the suction regime before the slope is subjected to rainfall. Laboratory and field tests have shown that vegetated soil could preserve suction of up to 20 kPa after rainfall, which is higher than that retained in bare soil (Lim et al. 1996; Simon and Collison 2002; Ng et al. 2013, 2014; Leung et al. 2015a, b). It may thus be imperative to consider the antecedent drying effects of plant transpiration before rainfall, when studying the effects of preserved suction on slope stability during rainfall.

This study aims to evaluate the performance of pole-supported slopes subjected to different rainfall conditions through centrifuge modelling. A novel live pole modelling technique developed by Ng and Yu (2014) was adopted to model both the mechanical reinforcement and hydrological effects of pole transpiration. In each test, responses of pore-water pressure (PWP) under two rainfall conditions (20- and 200-year return periods) were monitored. Transient seepage analyses were also carried out to investigate the antecedent drying effects of pole transpiration on the amount of suction preserved in a slope after rainfall.

Soil type

The soil type used was completely decomposed granite (CDG; silty sand, SM, according to the Unified Soil Classification System; ASTM D2487 2011b). The soil was air-dried and then sieved to discard any soil particles with diameter exceeding 5 mm, with the aim of

minimising any particle size effects in the centrifuge tests (Taylor 1995). The CDG comprised 2% gravel, 76% sand and 22% of fine particles. The specific gravity of the CDG was 2.60. Results from standard Proctor tests (ASTM D698-12e2 2012) show that the maximum dry density of CDG was 1870 kg/m^3 and the optimum water content was 13%.

The soil water retention curve (SWRC) and soil hydraulic conductivity function (SHCF) of the CDG were measured using the instantaneous profile method (IPM), following the procedures described by Ng and Leung (2012). All SWRCs and SHCFs (see Fig. 1) were fitted by van Genuchten's (1980) fitting equation. The fitting parameters are summarised in Fig. 1. It can be estimated from the drying SWRC (Fig. 1(a)) that the air-entry value of the CDG was ~1 kPa. A marked hysteresis loop can be observed clearly between the drying and wetting curves. The measured SHCF depicted in Fig. 1(b) was also hysteretic as expected. For a given suction, the hydraulic conductivity differed by almost one order of magnitude. The slight scattering of the SHCF data at suction ranging from 40 to 80 kPa was likely attributed to an error associated with the mathematical derivation of the non-linear hydraulic head profiles—a necessary step to determine the instantaneous profile of the hydraulic gradient in the IPM (Fluhler et al. 1976). Nevertheless, both the SWRCs and SHCFs were reasonably well fitted by van Genuchten's (1980) equation.

Following Krisdani et al. (2009), the saturated hydraulic conductivity (k_s) of the CDG was estimated using a statistical regression method together with a fitting equation (van Genuchten's (1980) equation in this case) to fit a set of measured SHCFs. The estimated k_s was be 1 x 10^{-8} m/s, which falls within the typical experimental range for this type of soil (i.e., 1.5 x 10^{-7} – 1.1 x 10^{-9} m/s; GEO 2000; Yin 2009; Ng et al. 2014).

Live poles

In order to model the hydrological effects of live pole in the centrifuge, a novel live pole

system developed by Ng and Yu (2014) was used. Fig. 2 shows the setup of the system consisting of a live pole, which is a branch cutting of a plant species, and a vacuum supply source. The top L_1 of the cutting with diameter D is inserted into a plastic tube and sealed with epoxy, while the remaining part of the cutting of length L_2 is buried in soil. The plastic tube delivers vacuum to the cutting, creating a negative pressure within the branch xylem. This establishes a hydraulic gradient between the surrounding soil and the cutting. According to Darcy's law, this gradient would drive water from the surrounding soil into the cutting. Any loss of soil moisture would induce soil suction.

In this study, branches of *Melastoma sanguineum* were used as live poles. This species is commonly used for slope rehabilitation and ecological restoration in tropical and subtropical regions of the world (Hau and Corlett 2003). Straight cuttings, or ones that were only slightly bent without forming large bifurcations, were screened for testing. The average D, L_1 and L_2 of cuttings adopted for testing were 4, 10 and 50 mm, respectively. When tested at 20 $\boldsymbol{g}$, the prototype dimensions were consistent with those typically found in the field (i.e., from 1 to 2 m in length and from 0.05 to 0.075 m in diameter; Steele et al. 2004; Wu et al. 2014). The cuttings were degassed by applying vacuum through the plastic tube. They were then submerged in de-aired water to prevent air from entering their xylem prior to testing.

The mechanical and hydraulic properties of *M. sanguineum* were characterised based on 15 screened cuttings. Results from mechanical tensile tests (ASTM E111-04 2010) show that Young's modulus (E) and tensile strength (σ_t) were 1252 ± 112 MPa and 14 ± 3 MPa, respectively. These values were close to those (E = 1500 MPa and σ_t = 15 MPa) reported by Khalilnejad et al. (2013) for the *Melastoma* species. These mechanical properties gave an axial rigidity (EA, where A is the cross-sectional area of a cutting) of 6×10^3 kPa-m^2 (prototype). k_s of each cutting was determined using a steady-state method suggested by Melcher et al. (2012). Each cutting was subjected to a known hydraulic gradient of 7.5, while

the rate of water flow across the cutting was monitored by a balance. At the steady state, k_s was found to be $5.3 \pm 0.3 \times 10^{-3}$ m/s (prototype). The properties of the cuttings, in both model and prototype scales, are summarised in Table 1. Ng and Yu (2014) found that their new live pole system using *M. sanguineum* was capable of creating sufficient suction in the field.

Centrifuge modelling

Test plan

Two centrifuge tests were performed at 20 ***g*** using a geotechnical beam centrifuge (4.2 m in radius; 400 ***g***-ton) facility at the Hong Kong University of Science and Technology. In the first test, denoted by R200, a scale model slope supported by the poles was subjected to an extreme rainfall event with an intensity of 108 mm/h for 2.5 h (prototype). This corresponded to a rainfall event with an equivalent return period of 200 years, based on the 26-year rainfall data (from 1984 – 2009) collected from Hong Kong (GEO 2007).

The second test, denoted by DW20, aimed to explore the antecedent drying effects of pole transpiration on PWP responses during rainfall. Three cycles of transpiration (defined as "drying") and rainfall (defined as "wetting") were simulated. In the three drying events, the transpiration duration was varied to create different amounts of suction before the subsequent wetting event. In the three wetting events, the rainfall was identical. In prototype scale, the rainfall also had an intensity of 108 mm/h (i.e., same as in Test R200), but with a shorter duration of 1 h. This rainfall pattern represented a less intense event (than the one in Test R200) and had a smaller return period of 20 years.

Model configuration and preparation

Fig. 3 shows the schematic setup of a centrifuge strong box containing the model slope for Test R200. All dimensions are expressed in model scale, unless stated otherwise. The slope

height was 7.7 m (prototype) and the slope angle was 40°. This slope angle was higher than those typically found in man-made slopes in the field to enable evaluating the effectiveness of using live poles to stabilise a steep slope. The slope geometry of Test DW20 (see supplementary data) was identical to that of Test R200.

Before compacting each model slope, silicone grease was pasted on all sides of the strong box. The grease helped minimise any friction and preferential flow of rainwater between the soil interface and all the boundaries of the strong box. Then, a supporting mould was fitted into the strong box to fix the slope geometry. In order to achieve 95% relative compaction (i.e., 1777 kg/m^3, the minimum density required for constructing fill slopes in Hong Kong; GEO (2000)), the CDG was mixed with water to a target water content of 16% according to the compaction curve obtained from standard Proctor tests. After compaction, the degree of saturation and volumetric water content of the compacted CDG were 80% and 25%, respectively. In total, 45 poles were inserted in nine rows of five spanning the entire model slope. The pole spacing was 1.4 m in prototype scale. All poles were installed perpendicularly to the slope surface. Poles installed in this fashion can be regarded as soil nails, which acted primarily in tension through the development of friction at the soil-pole interface. The pole spacing of 1.4 m was suggested by the Geotechnical Engineering Office (GEO 2011; 1.0 – 1.5 m), who established guidelines for satisfying the requirements of landscape works. Good contact was maintained between model poles and the surrounding soil during compaction.

In order to deliver an identical vacuum pressure to all poles, the plastic tube attached to each pole was connected to a vacuum delivery panel. The panel was connected to a vacuum chamber that was mounted outside the strong box. A solenoid valve was installed between the panel and the chamber so that the amount of vacuum to be applied can be remotely controlled during testing. In neither test was the water table controlled. The left and

bottom boundaries of each model slope were in contact with the strong box and thus were impermeable. After compaction, three rainfall devices designed by Zhang (2006) were mounted on the lid of each strong box for simulating different rainfall events during testing (see Fig. 3). The device was 340 mm in length and 200 mm in width. One of the devices was installed near the slope crest, while the other two were mounted near the sloping face. Each device had a water discharge panel consisting of 180 holes, each with a diameter of 0.5 mm. During rainfall simulation, water stored in the device was pressurised to control the rainfall intensity. Prior to testing, calibration showed that each device was able to create a uniform rainfall distribution over an area of 340 mm x 200 mm. The calibration also suggests that an intensity of 2160 mm/hr (model scale; i.e., equivalent to 108 mm/h at 20 $\boldsymbol{g}$ in prototype scale) can be produced when the water in the rainfall device is pressurized to about 75 kPa. By arranging the three rainfall devices as shown in Fig. 3, a uniform rainfall distribution can be achieved over the entire soil surface at the slope crest and sloping face. After installing the three rainfall devices, the box was covered with a lid to minimise any soil evaporation.

When modelling seepage events in a static centrifuge test, the scaling of seepage time is $1/N^2$ (Garnier et al., 2007). Under static conditions (i.e., zero soil acceleration), it is not necessary to consider time scaling with regard to soil movement (i.e., $1/N$). In other words, the viscosity of pore fluid need not be scaled to overcome the conflict between the scaling of time for seepage and dynamic loading. Water was thus used to simulate rainfall in this study.

Near the slope toe, a runoff collection frame (340 mm in length x 340 mm in width x 100 mm in height) was attached. In order to measure surface runoff during rainfall, the interfaces between the soil, the frame and the strong box were sealed with silicon grease to create a no-flow boundary condition at the slope toe. Hence, any surface water that had not infiltrated the slope would be collected and measured as surface runoff.

Instrumentation

Pore-water transducers (PPTs, Model: Druck PDCR81) were installed at various locations of the model slope (see Fig. 3) to monitor the responses of both positive and negative PWP. The sensing element (i.e., ceramic disk) in the PPTs measured 10 mm in length and 6 mm in diameter. Prior to installation, each PPT was subjected to a series of saturation and calibration procedures described by Zhou et al. (2006). Air dry tests (i.e., by leaving the PPTs exposed to air) showed that the PPTs were capable of measuring PWP down to -50 kPa reliably without any sign of hysteresis and cavitation. In the model slope, the PPT locations were chosen specifically for measuring the responses of PWP within and below the pole zone. Initially the PPT arrangement was identical in Tests R200 and DW20, but some PPTs malfunctioned during both centrifuge tests. Only the PPTs that worked fine are shown in Fig. 3.

Test procedures

In Test R200, the centrifuge was spun at 20 ***g***. At equilibrium, pole transpiration was simulated. The solenoid valve was opened to apply an identical vacuum pressure of 95 kPa to all 45 poles for 3.5 h (2 months in prototype scale). Then, the valve was closed to stop the simulation of transpiration, followed by a rainfall event that lasted for 22 s (2.5 h in prototype scale) with an intensity of 2160 mm/h (108 mm/h in prototype scale). When no further change in PWP was observed in all PPTs after rainfall, the centrifuge was spun down.

In Test DW20, three drying-wetting cycles were applied to the model slope at 20 ***g***. The first cycle was a repetition of Test R200 (i.e., applying an identical vacuum pressure of 95 kPa for 3.5 h) but with a shorter rainfall duration (9 s; 1 h in prototype scale) during the wetting event. In the second cycle, transpiration was simulated again but for 1.8 h only (one month in prototype scale), half the amount of time as that applied in the first cycle to create a different initial suction condition. Then, a rainfall event with a return period of 20 years was

applied again. The test condition for the third cycle was identical to that for the first cycle. There was no time lag between each drying-wetting cycle.

Centrifuge test results

Slope hydrology under an extreme rainfall event

Fig. 4 shows the measured variations in PWP during pole transpiration in Test R200 after the model slope had reached the equilibrium at 20 ***g***. It can be seen that when vacuum was applied to the poles, the PWP dropped immediately at all PPT locations. This was likely the undrained response of the CDG when the water uptake rate of live poles exceeded the rate of water flow in the soil. Subsequently, all PPTs showed partial recovery in PWP due to the dissipation of excess PWP generated by the instantaneous vacuuming. Thereafter, a reduction in PWP was observed again, but at a much slower rate. The measured decreases in PWP (or increase in suction) were attributed to the continuous removal of soil moisture due to the water uptake of the poles. At the end of the drying event, the suction ranged between 15 and 35 kPa, depending on the height at which measurements were taken. It appears that the higher up the slope, the higher the suction would be. This may be because in addition to the pole water uptake, there was lateral water flow across the slope. For PPTs installed at relatively low elevations such as P6 (near the slope toe), any suction induced by adjacent live poles might be reduced by water flow from higher up the slope.

After the extreme rainfall event, 62% of the total applied rainfall was discharged as runoff (i.e., 38% of rainfall infiltrated the slope). Suction induced in the previous drying period disappeared after the rainfall. The PWP near the slope toe (P6) attained its peak of +8.5 kPa momentarily during rainfall. It dropped to zero in about eight days after the rainfall. The observed significant increase in positive PWP near the slope toe was probably attributed to the rise of the groundwater table due to rainfall infiltration and downward seepage from

the upper portion of the slope. As rainfall stopped, the groundwater might have receded leading to the decrease in PWP. At the end of the test, the slope was stable, without showing any sign of collapse. A careful inspection revealed negligible soil erosion at the slope toe.

Effects of pole transpiration duration on PWP response

Fig. 5 shows the time history of PWP during the three drying-wetting cycles in Test DW20. The PWP responses observed during the first drying cycle were similar to those seen in Test R200. After a less extreme rainfall event, suction also decreased, but much less significantly than after the heavier rainfall in Test R200. The shallower PPTs (i.e., P1 and P2) showed a greater drop in suction (i.e., by 15 kPa). The measured suction changes recorded at P3 and P4 was significantly smaller than other PPTs. This is expected because upon rainfall infiltration, the hydraulic gradient was greater at shallower depths, causing more significant changes in suction. At the end of this rainfall event, a substantial amount of suction (10 to 15 kPa) was preserved at all measurement depths. Similar to Test R200, the slope in Test DW20 remained stable after one drying-wetting cycle.

After the first cycle, pole transpiration was simulated again in the second drying cycle but with the duration shortened by half. According to the summary of test data shown in Table 2, the peak induced suction at the end of the first and second drying cycles differed by no more than 2 kPa for all four PPTs. This might be attributed to the hysteretic SWRC and SHCF of the CDG (Fig. 1). During the second drying cycle, the CDG might follow scanning curves that are different from those experienced in the first cycle.

Table 2 also reveals that the differences in the minimum suction at the end of the first and second wetting cycles were less than 1 kPa for P2, P3 and P4. However, after rainfall, the drop in suction in the second cycle was generally greater than that in the first cycle. When pole transpiration was simulated again for a longer duration during the third drying cycle,

higher peak suctions (14 – 30 kPa) were induced than those (10 – 23 kPa) recorded during the two previous drying events. Moreover, the test results in Fig. 5 seemed to show that at the end of the second and third drying cycles, the suctions were the same as they would have been had the rainfall event never occurred. This implies that the slopes might have been headed toward the steady-state condition that was temporarily interrupted by the rainfall. This might be because the drops in suction during all wetting events followed scanning wetting paths. In the subsequent drying events, as a result of pole transpiration, suction recovered following primary drying curves and possibly expanding the suction-increase (SI) yield surface (Wheeler et al. 2003). As the same rainfall pattern occurred again for the third wetting cycle, suction also decreased, but on this occasion, the suction preserved was higher than those recorded in the previous two cycles (Table 2). This means that even though the rainfall event was identical in all three cycles, the suction responses can differ dramatically, depending on the duration of the antecedent drying event of pole transpiration. No slope failure was observed after the second and third drying-wetting cycles.

The effect of antecedent drying on the PWP response was more prominent from the PWP profiles in Fig. 6. Due to pole transpiration in the top 1 m of the slope, a higher amount of PWP was always induced at shallower depths before rainfall in all three drying cycles. After rainfall, suction dropped more substantially at shallower depths (around 15 kPa) than it did at greater depths (less than 5 kPa). This is likely because the hydraulic gradient was much higher at shallower depths as rainfall took place at the slope surface. The rainwater infiltration thus mainly affected the shallower soil, causing the observed greater changes in suction. Similarly, a rather uniform suction distribution was obtained after the third wetting cycle. However, the magnitude of suction (i.e., ~10 kPa) was two times higher than that observed in the previous two wetting cycles (i.e., ~ 5 kPa). This is likely because of the significantly higher pole-induced suction during the third drying cycle, which may have led

to a reduction in hydraulic conductivity (refer to Fig. 1(b)) and hence the observed amount of infiltration. More importantly, the amount of suction preserved seemed to be proportional to the suction induced by pole transpiration before rainfall, although it can also be affected by the duration of both the drying and rainfall events.

Numerical modelling

In order to further interpret the centrifuge test data, numerical analyses were performed to study the antecedent drying effects of pole transpiration on the amount of suction preserved after rainfall. Transient seepage analyses were conducted to establish the correlation between suction before and after rainfall, which was then compared with the centrifuge measurements. Since the slope was stable during the tests, stability analysis was not conducted in this study.

The finite element software, SEEP/W (Geo-Slope Int. 2009), was used to simulate transient seepage in unsaturated soil. The governing equation is based on mass conservation and Darcy's law, and it is generally referred to as Richard's equation:

$$k\left[\frac{\partial}{\partial x}\left(\frac{\partial H}{\partial x}\right)+\frac{\partial}{\partial y}\left(\frac{\partial H}{\partial y}\right)\right]+Q=m_w\gamma_w\frac{\partial H}{\partial t} \quad (1)$$

where H is total head; k is SHCF, which is a function of PWP (u_w); m_w is the slope of an SWRC (also known as the water storage capacity); γ_w is the unit weight of water; Q is applied boundary flux; t is elapsed time; and x and y are the 2D coordinate system. Eqn (1) assumes that a change in PWP would not alter the soil volume. It is a fair assumption for CDG as previous experiments (Leung and Ng 2015) have shown that densely-compacted decomposed soil with a high coarse content, like CDG, exhibits negligible volume change for suctions less than 100 kPa. Fig. 7 shows the adopted finite element mesh, which has the same prototype dimensions and boundary conditions as the model slope tested in the centrifuge. In order to compare the measured data and computed results, the rainfall flux was applied on the horizontal ground surface at the slope crest and the sloping face in the numerical models.

When the rainfall intensity is greater than the saturated hydraulic conductivity, the amount that can potentially infiltrate the ground is assumed to be equal to the saturated hydraulic conductivity. The remaining portion disappears as runoff. When runoff takes place, it is assumed by SEEP/W that the pressure head at the soil surface is set to be zero.

In order to establish the correlation between suction before and after rainfall, five series of transient analyses were conducted, considering five different initial suctions (i.e., 10, 20, 40, 60 and 100 kPa) uniformly distributed within the live pole zone of the slope (i.e., the layer of soil supported by live poles). These values represent different suction regimes after a vegetated slope has been subjected to different durations of transpiration before rainfall. This range of initial suctions covered the values observed in the two centrifuge tests (i.e., 16 – 24 kPa; presented later). Transpiration-induced suction of up to 100 kPa was not uncommon in the CDG tested in this study. Garg et al. (2015) observed similar levels of transpiration-induced suction in their experiments. For each initial suction regime, five different rainfall patterns were imposed on the slope (i.e., 25 analyses in total). The first four patterns involved four different rainfall intensities, 64, 108, 135 and 145 mm/h, all with the same duration of 1 h. These patterns correspond to the return periods of 2, 20, 100 and 200 years, respectively. The last pattern was a rainfall event with an intensity of 108 mm/h but lasting for a longer duration of 2.5 h, which gives a return period of 200 years. For modelling rainfall infiltration, the wetting SWRC and SHCF (Fig. 1) were input for all cases.

Influence of pole transpiration and rainfall on slope hydrology

Fig. 8 correlates the measured suction preserved (at 1 m depth by P4 in Test R200 and by P2 in Test DW20) after rainfall with the measured suction induced by pole transpiration right before rainfall in both centrifuge tests. Simulation results obtained from the 25 transient seepage analyses are also included in Fig. 8 for comparison. The centrifuge datasets appeared

to follow the predicted trend lines, especially the data obtained from Test DW20. Some studies (Tami et al. 2004; Yang et al. 2012) have revealed that the measured variation in soil suction is larger than that predicted by a non-hysteretic model at both the steady and transient states. Model slope experiments performed by Tami et al. (2004) show that drying and wetting can simultaneously occur in different parts of the soil. Such a combined process cannot be captured by a non-hysteretic model (Yang et al. 2012). The measurements and predictions both consistently showed that the suction preserved after rainfall was higher when the suction induced by the previous drying event was higher. Depending on the rainfall intensity and duration, 5% (for a 200-year rainfall) to 50% (for a 2-year rainfall) of suction can be preserved in the CDG. This suggests that additional suction induced by transpiration enhanced the ability of the soil to preserve suction in subsequent rainfall events.

Fig. 8 also shows that the ability of the CDG to preserve suction after rainfall was not only dependent upon the amount of suction induced by pole transpiration, but was also related to the rainfall patterns. For the same given rainfall duration of 1 h, the amount of suction preserved decreased as the intensity of rainfall increased. Interestingly, simulations suggest a critical rainfall intensity (i.e., 135 mm/h; 100-year return period in this case). Beyond this threshold (e.g., 145 mm/h; 200-year return period), the CDG had the same suction retention capacity, regardless of the amount of suction induced before rainfall. This is because the slope had already reached its infiltration capacity with the 100-year rainfall. Any further increases in rainfall intensity led to the same amount of infiltration.

For the same intensity of 108 mm/h, extending the rainfall duration from 1 to 2.5 h led to a substantial drop in suction. This is because the rainwater infiltrated the soil for a longer period of time. The gradient of the correlation for the 2.5 h case was much gentler than that for the 1 h case. This means that suction preserved in the CDG after rainfall was less dependent upon the amount of suction previously induced. Thus live pole transpiration could

help reduce infiltration and hence preserve adequate suction in CDG to withstand certain rainfall conditions. However, the benefits of live pole transpiration would be diminished as the intensity and duration of rainfall increased.

Effects of rainfall infiltration on transpiration-induced suction

Fig. 9(a) shows the variations in cumulative infiltration (expressed in m^3 per one meter width of slope) with different initial suctions before rainfall. The computed infiltration under a rainfall intensity of 108 mm/h for 2.5 h was by far the highest for any given initial suction. The rainfall duration in this case was 2.5 times longer than that in all other cases. As have been reported by Ng and Shi (1998) and Rahardjo et al. (2001), a long-duration, low-intensity rainfall event would result in a greater amount of infiltration than a short-duration, high-intensity event. The computed infiltration (~40 m^3/m) was higher than the measurement from Test R200 (~33 m^3/m). This means that the computed infiltration was 42%, compared with the measured value of 38%. The discrepancy may be considered to be acceptable.

The computed results showed a consistent decrease in infiltration as the initial suction increased. In order to better understand this trend, the water storage capacity (m_w) along the wetting path is determined, where m_w is the gradient of the wetting SWRC, describing the increase in volumetric water content (VWC) under a given change in suction. Following the SWRC equation proposed by van Genuchten (1980), m_w can be derived as follows:

$$m_w(\psi) = -\frac{d\theta}{d\psi} = \frac{-nm(\theta_s-\theta_r)(a\psi)^n}{[1+(a\psi)^n]^{m+1}} \quad (2)$$

where θ, θ_s and θ_r are volumetric water content (VWC), saturated VWC and residual VWC, respectively; a, n and m are fitting parameters of the SWRC model proposed by van Genuchten (1980); and ψ is suction. The values of m_w at different initial suctions are also depicted in Fig. 9(a). As the initial suction increased, m_w decreased exponentially. This means that any suction change in the higher suction range would lead to a smaller VWC reduction.

The lower water storage capacity and lower hydraulic conductivity (see also Fig. 1(b)) at high initial suction thus resulted in a smaller amount of rainfall infiltration.

The effects of m_w on suction drop at 1 m depth under the five different rainfall events are compared in Fig. 9(b). In all cases, the amount of suction drop decreased exponentially as m_w increased. According to Eqn (2), a smaller m_w means that for a given increase in VWC due to rainfall infiltration, the corresponding reduction in suction would be greater. This explains why higher initial suction (i.e., lower m_w) before rainfall would result in a greater drop in suction and hence more suction retained as observed in Fig. 8. The markedly greater drop in suction for the case with rainfall intensity of 108 mm/h and duration of 2.5 h in Fig. 9(b) was because of the greater amount of infiltration (see also Fig. 9(a)).

In Test R200, the initial suction before rainfall was 16 kPa, which corresponded to an m_w of 0.0221 kPa^{-1}. After the rainfall event, no suction was preserved (i.e., suction drop was 16 kPa). This measurement was 25% higher than those found in all other cases (9 – 12 kPa; see Fig. 9(b)). This may be attributed to the underestimation of infiltration due to the use of non-hysteretic model in the SEEP/W analyses.

Summary and conclusions

This study investigates the hydrological effects of transpiration of live poles to the slope hydrology. Two centrifuge model tests were carried out by subjecting pole-supported silty sand slopes to rainfall featuring return periods of 20 and 200 years. A novel live pole modelling technique was adopted. Branch cuttings of a real plant (*Melastoma sanguineum*) that is commonly used for slope rehabilitation were selected as the poles so that the mechanical properties including tensile strength and elastic modulus could be modelled correctly. By connecting each cutting to a vacuum source, the effects of live pole transpiration was simulated. The centrifuge test results show that the live pole modelling

technique could induce suction of up to 35 kPa.

After rainfall with a return period of 20 years (108 mm/h for 1 h in prototype scale), 5 – 10 kPa of suction was preserved in the slope. The amount of suction preserved after rainfall was dependent upon the amount of suction induced by pole transpiration before rainfall. This is because the suction induced by pole transpiration reduced the soil water storage capacity and hydraulic conductivity, which in turn reduced the rainfall infiltration. The ability of the silty sand to preserve suction was identified to be a function of the rainfall pattern. For a given rainfall intensity of 108 mm/h, extending the rainfall duration from 1 to 2.5 h (i.e., the return period becomes 200 years) reduced the ability of the silty sand to preserve suction because more infiltration took place. On the other hand, for a given rainfall duration (i.e., 1 h), there existed a critical rainfall intensity (135 mm/h), beyond which the ability of the silty sand to preserve suction remained constant. This is because the silty sand had reached its infiltration capacity at the critical rainfall intensity and any further increases in intensity simply resulted in surface runoff.

Acknowledgements

The authors received a research grant (HKUST6/CRF/12R) from by the Research Grants Council of the Government of the Hong Kong SAR and another one (2012CB719805) from the Ministry of Science and Technology of the People's Republic of China under the National Basic Research Program (973 Program). The second author would also like to acknowledge the funding provided by the EU FP7 Marie Curie Career Integration Grant (CIG) under the project “BioEPIC slope”, as well as research travel support from the Northern Research Partnership (NRP). The forth author also acknowledge the “Hong Kong-Scotland Partners in Post-Doctoral Research” (S-HKUST601/15) provided by the Research Grants Council of Hong Kong SAR and the Scottish Government.

References

ASTM D698-12e2 (2012). "Standard Test Methods for Laboratory Compaction Characteristics of Soil Using Standard Effort (12, 400 ft-lbf/ft^3 (600 kN-m/m^3).", West Conshohocken, PA.

ASTM E111-04. (2010). "Standard Test Method 469 for Young's Modulus, Tangent Modulus, and Chord Modulus.", West Conshohocken, PA.

ASTM D2487 (2011b). "Standard practice for classification of soils for engineering purposes (unified soil classification system).", West Conshohocken, PA.

Fluhler, H., M. S. Ardakani, and L. H. Stolzy. (1976). "Error propagation in determining hydraulic conductivities from successive water content and pressure head profiles." *Soil Sci. Soc. Am. J.*, 40, 830–836.

Garg, A., Leung, A. K., and Ng, C. W. W. (2015). "Transpiration reduction and root distribution functions for a non-crop species *Schefflera heptaphylla*." *Catena*, 135, 78–82.

Garnier, J., Gaudin, C., Springman, S. M., Culligan, P. J., Goodings, D., Konig, D., Kutter, B., Phillips, R., Randolph, M. F., and Thorel, L. (2007). "Catalogue of scaling laws and similitude questions in geotechnical centrifuge modelling." *Int. J. of Phys. Model. in Geotech.*, 3, 1–23.

Geotechnical Engineering Office (2000). *Guide to retaining wall design*. Geoguide 1. Geotechnical Engineering Office (GEO), Civil Engineering and Development Department, The Government of the Hong Kong SAR.

Geotechnical Engineering Office (GEO) (2007). *Frequency analysis of extreme rainfall values.* GEO Report No. 261. Geotechnical Engineering Office, Civil Engineering and Development Department, HKSAR.

Geotechnical Engineering Office (GEO) (2011). *Technical Guidelines on landscape treatment for slopes.* GEO Publication No. 1/2011. Geotechnical Engineering Office,

494 Civil Engineering and Development Department, HKSAR.
495 Geo-Slope International Ltd. (2009). *Seepage Modeling with SEEP/W*. An Engineering
496 Methodology, 4th Edn
497 Hau, B. C., and Corlett, R. T. (2003). "Factors affecting the early survival and growth of
498 native tree seedlings planted on a degraded hillside grassland in Hong Kong, China."
499 *Restor. Ecol.*, 11, 483–488.
500 Kamchoom, V., Leung, A. K., and Ng, C. W. W. (2014). "Effects of root geometry and
501 transpiration on pull-out resistance." *Géotechnique Lett*., 4, 330–336.
502 Khalilnejad, A., Ali, F., Hashim, R., and Osman, N. (2013). "Finite-element simulation for
503 contribution of matric suction and friction angle to stress distribution during pulling-out
504 process." *Int. J. of Geomech*., 13(5), 527–532.
505 Krisdani, H., Rahardjo, H., and Leong, E.-C. (2009). Use of instantaneous profile and
506 statistical methods to determine permeability functions of unsaturated soils. *Can.*
507 *Geotech. J.*, 46(7), 869–874.
508 Leung, A. K., and Ng, C. W. W. (2015). "Field investigation of deformation mechanisms and
509 stress mobilisation in a soil slope." *Landslides*. In press.
510 Leung, A. K., Garg, A., and Ng, C. W. W. (2015a). "Effects of plant roots on soil-water
511 retention and induced suction in vegetated soil." *Eng. Geol*., 193, 187-197.
512 Leung, A. K., Garg, A., Coo, J. L., Ng, C. W. W., and Hau, B. C. H. (2015b). "Effects of the
513 roots of Cynodon dactylon and Schefflera heptaphylla on water infiltration rate and soil
514 hydraulic conductivity." *Hydrol. Process*. In press
515 Lim, T. T., Rahardjo. H., Chang, M. F., and Fredlund, D. G. (1996). "Effect of rainfall on
516 matric suctions in a residual soil slope." *Can. Geotech. J.*, 33(4), 618–628.
517 Melcher, P. J., Michele H. N., Burns, M. J., Zwieniecki, M. A., Cobb, A. R., Brodribb, T. J.,
518 Choat, B., and Sack, L. (2012). "Measurements of stem xylem hydraulic conductivity in

519 the laboratory and field method." *Method in Ecol. Evol*., 3(4), 685-694.
520 Ng, C. W. W., and Leung, A. K. (2012). "Measurements of drying and wetting permeability
521 functions using a new stress-controllable soil column." *J. of Geotech. Geoenviron. Eng., ASCE*, 138(1), 58-65.
523 Ng, C. W. W., and Shi, Q. (1998). "A numerical investigation of the stability of unsaturated
524 soil slopes subjected to transient seepage." *Comput. Geotech.*, 22(1), 1–28.
525 Ng, C. W. W., and Yu, R. (2014). "A novel technique to model water uptake by plants in
526 geotechnical centrifuge." *Géotechnique Lett*., 4(1), 244-249.
527 Ng, C. W. W., Leung, A. K., and Woon, K. X. (2014). "Effect of soil density on grass-
528 induced suction distributions in compacted soil subjected to rainfall." *Can. Geotech. J.*, 51(3), 311-321.
530 Ng, C. W. W., Woon, K. X., Leung, A. K., and Chu, L. M. (2013). "Experimental
531 investigation of induced suction distributions in a grass-covered soil." *Ecol. Eng.*, 52, 219-223.
533 Rahardjo, H., Li, X. W., Toll, D. G., and Leong, E. C. (2001). "The effect of antecedent
534 rainfall on slope stability." *Geotech. and Geol. Eng.*, 19, 371–399.
535 Sidle, R. C., Pearce, A. J., and O'Loughln, C. L. (1985). "Hillslope stability and land use.
536 American Geophysical Union." *Water Resour. Monogr.*, 11. Washington DC.
537 Simon, A., and Collison, A. (2002). "Quantifying the mechanical and hydrologic effects of
538 riparian vegetation on strembank stability." *Earth Surf. Process. Landf.*, 27(5), 527–546.
539 Sonnenberg, R., Bransby, M. F., Bengough, A. G., Hallett, P. D., and Davies, M. C. R.
540 (2012). "Centrifuge modelling of soil slopes containing model plant roots." *Can. Geotech. J.*, 49(1), 1-17.
542 Sonnenberg, R., Bransby, M. F., Hallett, P. D., Bengough, A. G., Mickovski, S. B., and
543 Davies, M. C. R. (2010). "Centrifuge modelling of soil slopes reinforced with vegetation."

544 *Can. Geotech. J.*, 47(12), 1415-1430.
545 Steele, D., MacNeil, D., Barker, D., and McMahon, W. (2004). "The use of live willow poles
546 for stabilising highway slopes." *TRL Report no. 619*, TRL.
547 Tami, D., Rahardjo, H., and Leong, E. C. (2004). "Effects of hysteresis on steady-state
548 infiltration in unsaturated slopes." *J. of Geotech. Geoenviron. Eng., ASCE*, 130(9), 956–
549 967.
550 Taylor, R. N. (1995). *Geotechnical Centrifuge Technology*. Taylor and Francis.
551 van Genuchten, M. T. (1980). "A closed-form equation for predicting the hydraulic
552 conductivity of unsaturated soils." *Soil Sci. Am. J.*, 44(5), 892-898.
553 Wheeler, S. J., Sharma, R. S., and Buisson, M. S. R. (2003). "Coupling of hydraulic
554 hysteresis and stress–strain behaviour in unsaturated soils." Géotechnique, 53(1), 41-54.
555 Wu, T., Kokesh, C., Trenner, B., and Fox, P. (2014). "Use of Live Poles for Stabilization of a
556 Shallow Slope Failure." *J. Geotech. Geoenviron. Eng., ASCE*., 140(10), 05014001.
557 Yang, C., Sheng, D., and Carter, J. P. (2012). "Effect of hydraulic hysteresis on seepage
558 analysis for unsaturated soils." *Comput. Geotech.*, 41, 36–56.
559 Yin, J.-H. (2009). "Influence of relative compaction on the hydraulic conductivity of
560 completely decomposed granite in Hong Kong." *Can. Geotech. J.*, 46, 1229–1235.
561 Zhang, M. (2006). *Centrifuge modelling of potentially liquefiable loose fill slopes with and
562 without soil nails*. PhD thesis, The Hong Kong University of Science and Technology,
563 Hong Kong SAR.
564 Zhou, Z. B. R., Take, W. A., and Ng, C. W. W. (2006). "A case study in tensiometer
565 interpretation: centrifuge modelling of unsaturated slope behaviour." *Proc. of the 4th Int.
566 Conf. on Unsaturated Soils 2006*. Ed. by G. A. Miller, C. E. Zapata, S. L. Houston, and D.
567 G. Fredlund, Arizona, United States, 2 – 6 April, 2006, pp. 2300-2311.
568

569 **LIST OF CAPTIONS**

570 **Table captions**

574

575 **Figure captions**

590

591 Table 1. Summary of relevant scaling laws used in this study

Parameter	**Dimension**	**Scaling factor**	**Model scale**	**Prototype scale**
Geometry of model live poles				
Length (mm)	L	$1/N$	50	1000
Diameter (mm)	L	$1/N$	4	80
Cross-sectional area (m^2)	L^2	$1/N^2$	1.25×10^{-5}	5.03×10^{-3}
Material properties of model live poles				
Tensile strength (kPa)	M/LT^2	1	1.4×10^4	1.4×10^4
Young's modulus (kPa)	M/LT^2	1	1.2×10^6	1.2×10^6
Axial rigidity, *EA* (kPa-m^2)	ML/T^2	$1/N^2$	15	6.0×10^3
Hydraulic conductivity (m/s)	L/T	N	0.106	5.3×10^{-3}
Seepage				
Seepage velocity (m/s)	L/T	N	2.0×10^{-6}	1.0×10^{-7}
Seepage time (s)	T	$1/N^2$	Depends on test	
Pore-water pressure (kPa)	M/LT^2	1		
Rainfall intensity (mm/h)	L/T	N	2160	108
Rainfall duration	T	$1/N^2$	22 s or 9 s	2.5 h or 1 h

592

593 Table 2. Summary of the measured values of suction in Test DW20 from the pore pressure
594 transducers P1, P2, P3 and P4.

	Measured suction (kPa)			
Test conditions of DW20	**P1**	**P2**	**P3**	**P4**
After 1st drying	20.6	16.5	13.7	8.8
After 1st wetting	10.6	5.0	4.5	3.4
Suction drop after rainfall (kPa)	10	11.5	9.2	5.4
After 2nd drying	22.6	18.2	15.6	10.3
After 2nd wetting	6.2	5.0	4.0	3.8
Suction drop after rainfall (kPa)	17.4	13.2	11.6	6.5
After 3rd drying	30.5	22.8	19.9	14.1
After 3rd wetting	14.3	8.6	9.6	8.6
Suction drop after rainfall (kPa)	16.2	14.2	10.3	5.5

595

596

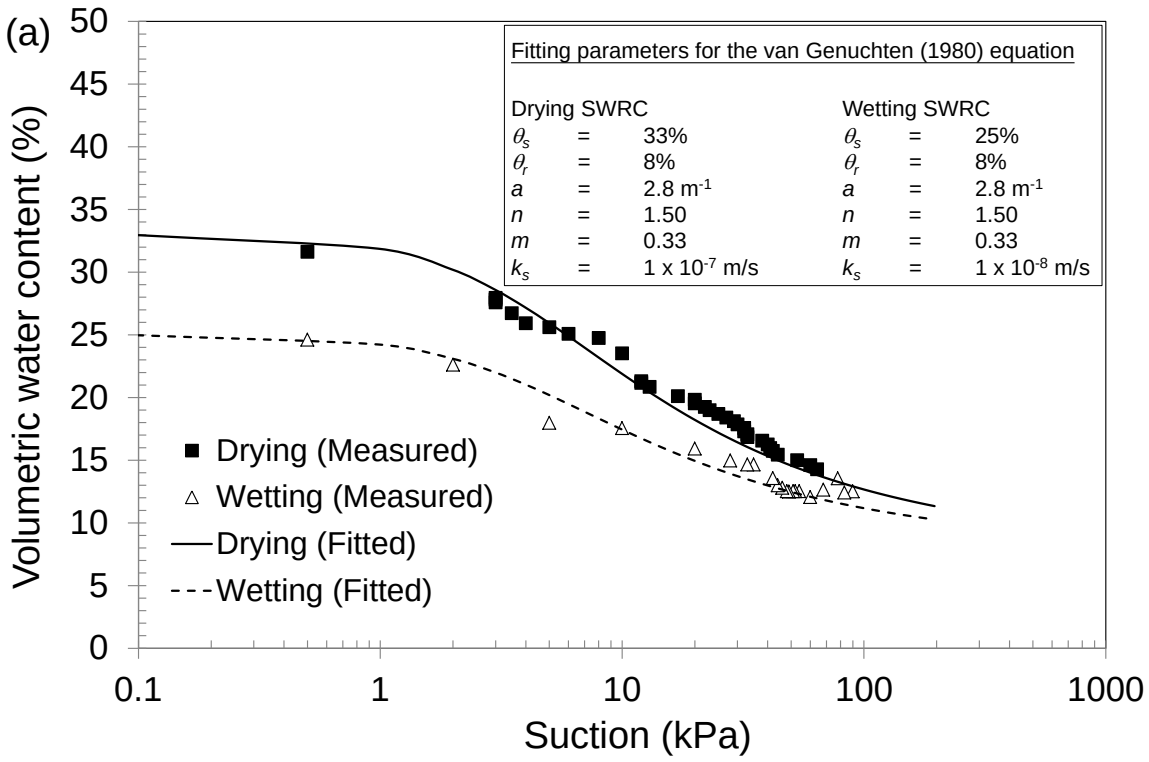

597

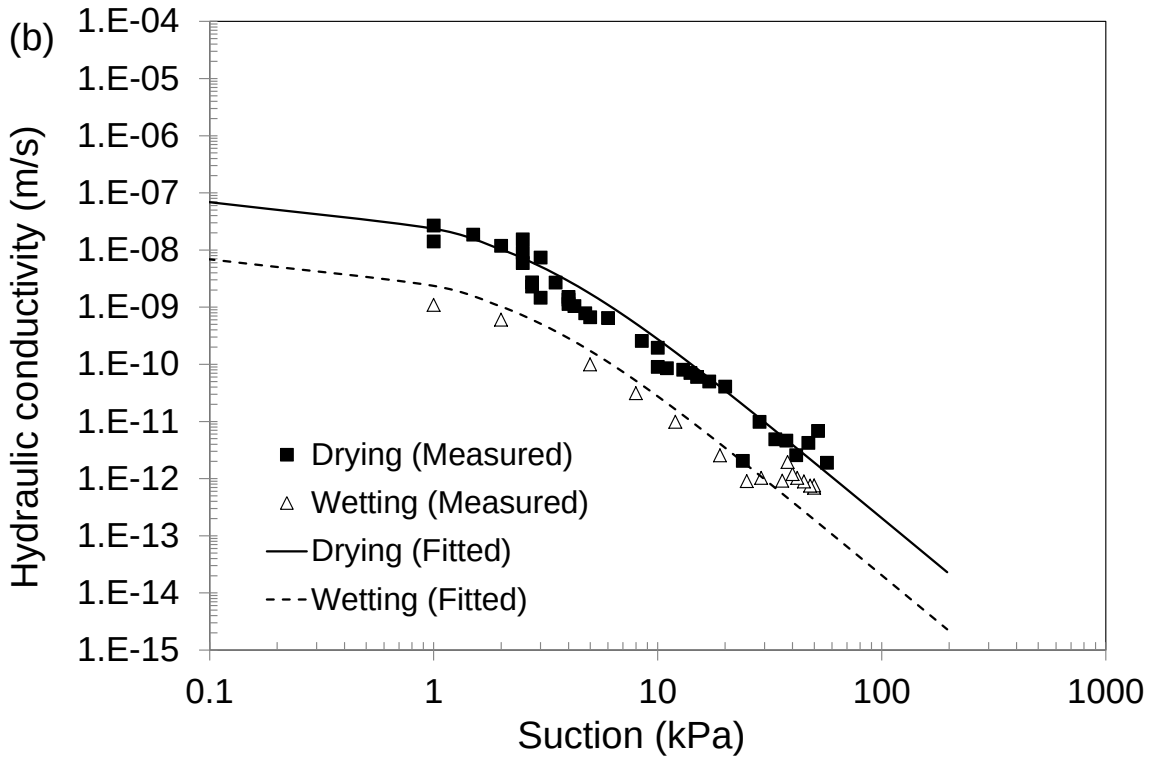

598

599

600 **Fig. 1** Measured and fitted hydraulic properties of CDG: (a) SWRC and (b) SHCF

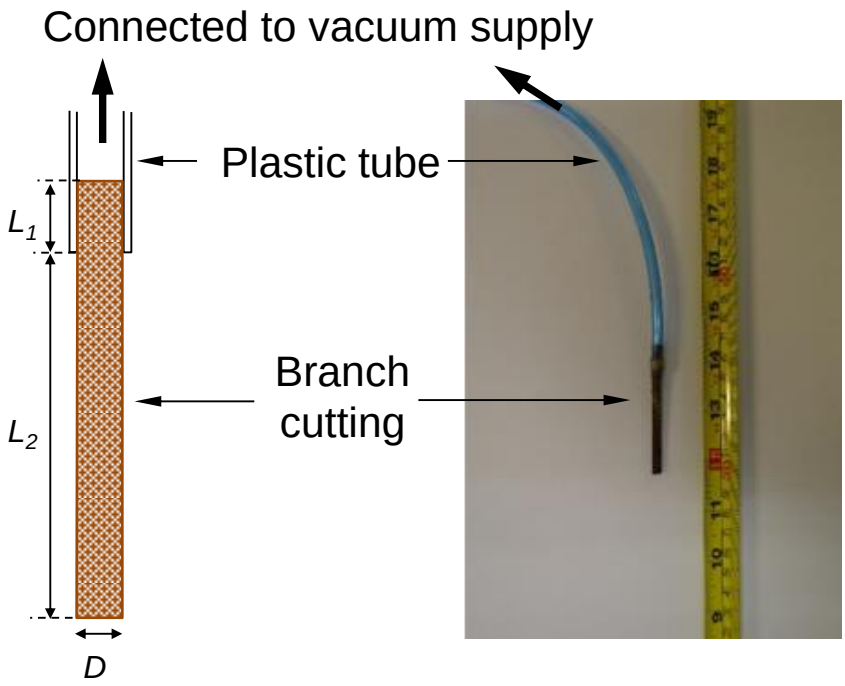

601

602 **Fig. 2** Schematic diagram and image of the set-up of a model live pole (Ng and Yu 2014)

603

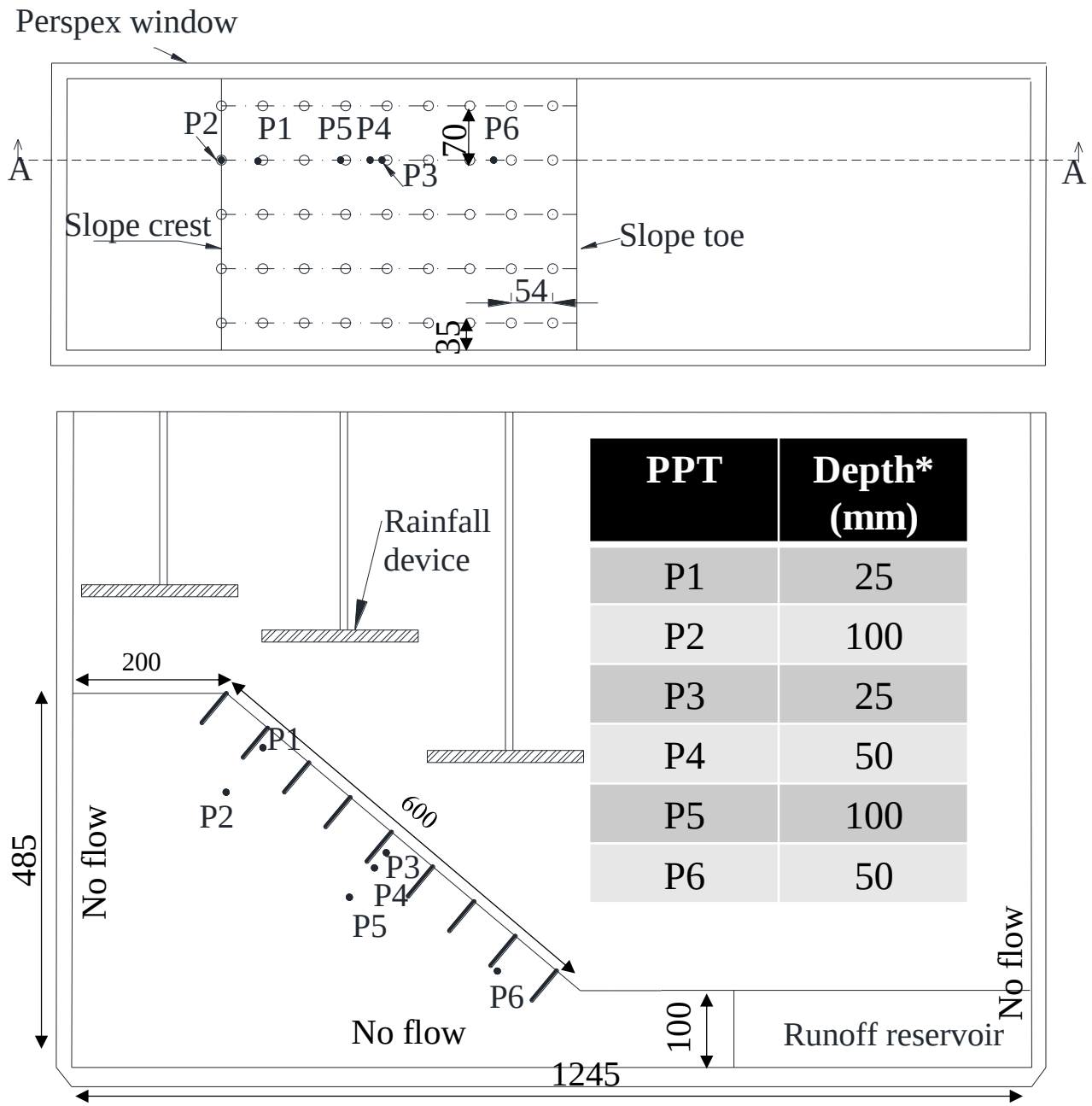

PPT	Depth* (mm)
P1	25
P2	100
P3	25
P4	50
P5	100
P6	50

604

605

606 **Fig. 3** Plan view (upper) and elevation view (lower) of the model box for Test R200

607

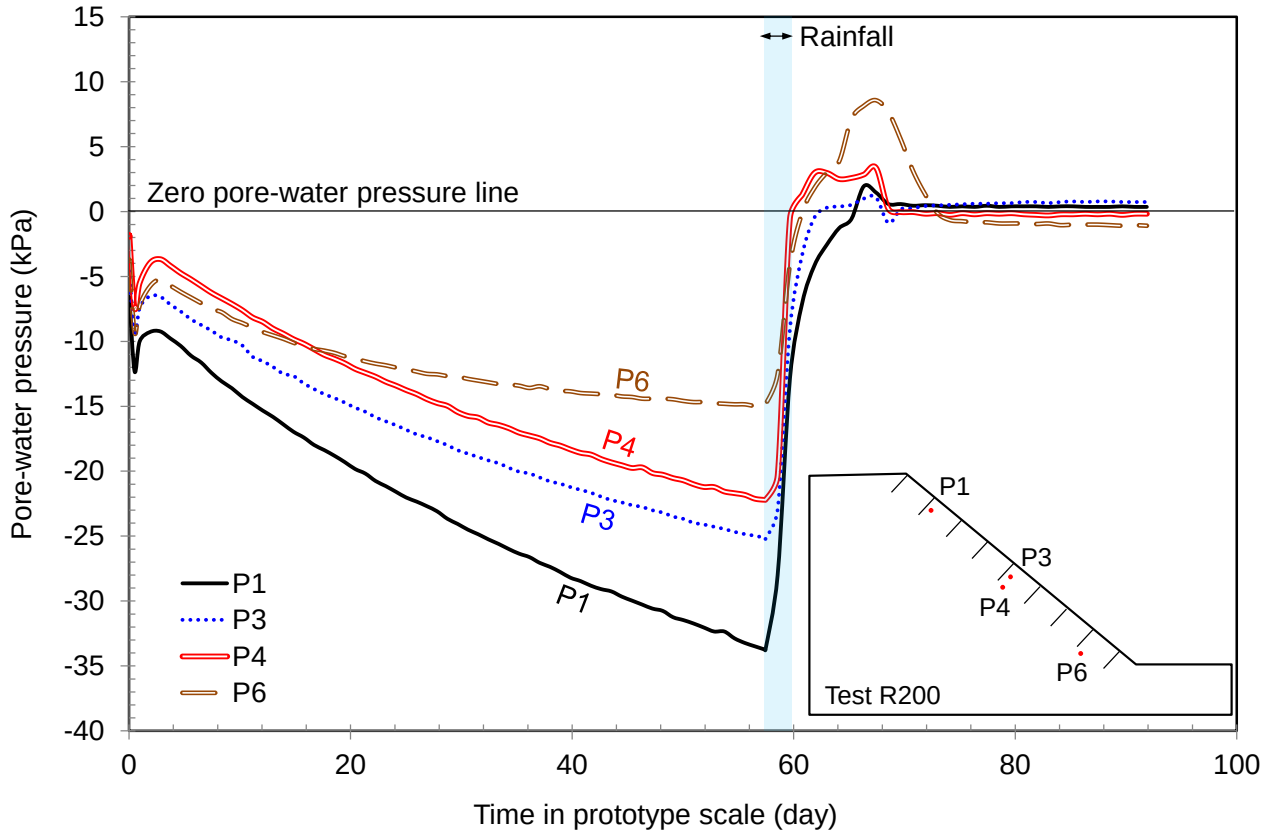

608

609 **Fig. 4** Measured variations in PWP with time during live pole transpiration in Test R200

610

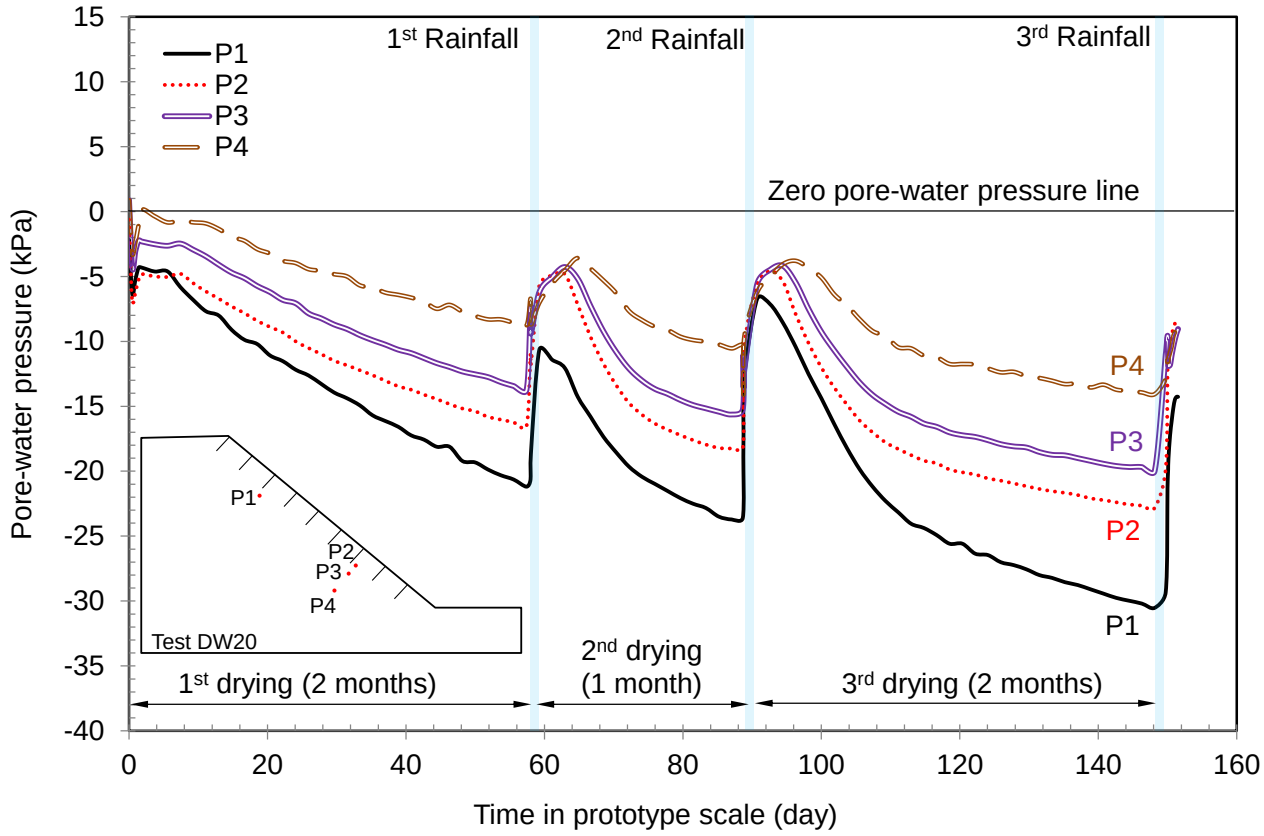

611

612 **Fig. 5** Measured responses of PWP during three cycles of live pole transpiration (drying) and

613 rainfall infiltration (wetting) in Test DW20

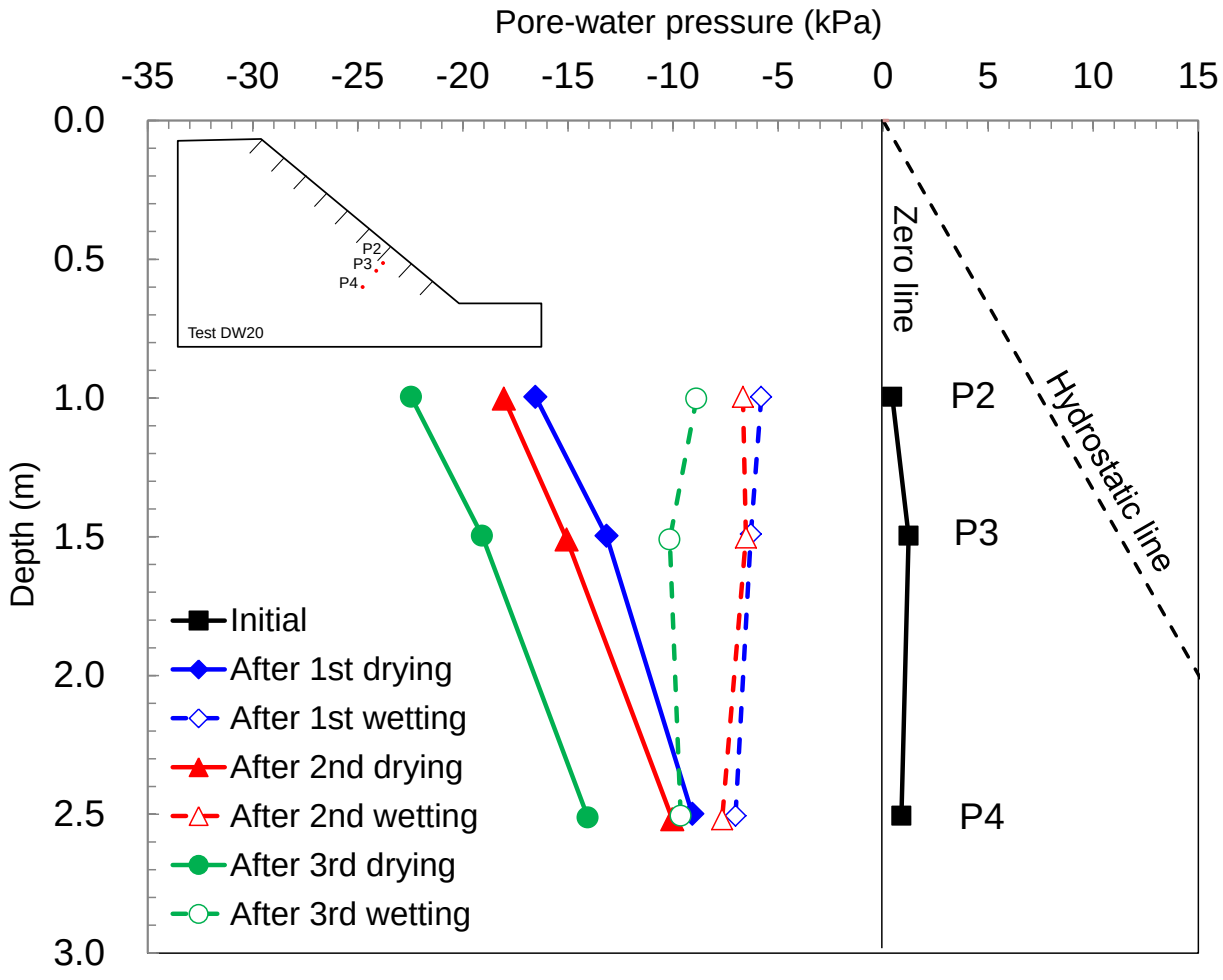

614

615 **Fig. 6** Distributions of measured PWP along depth before and after three rainfall events in

616 Test DW20

617

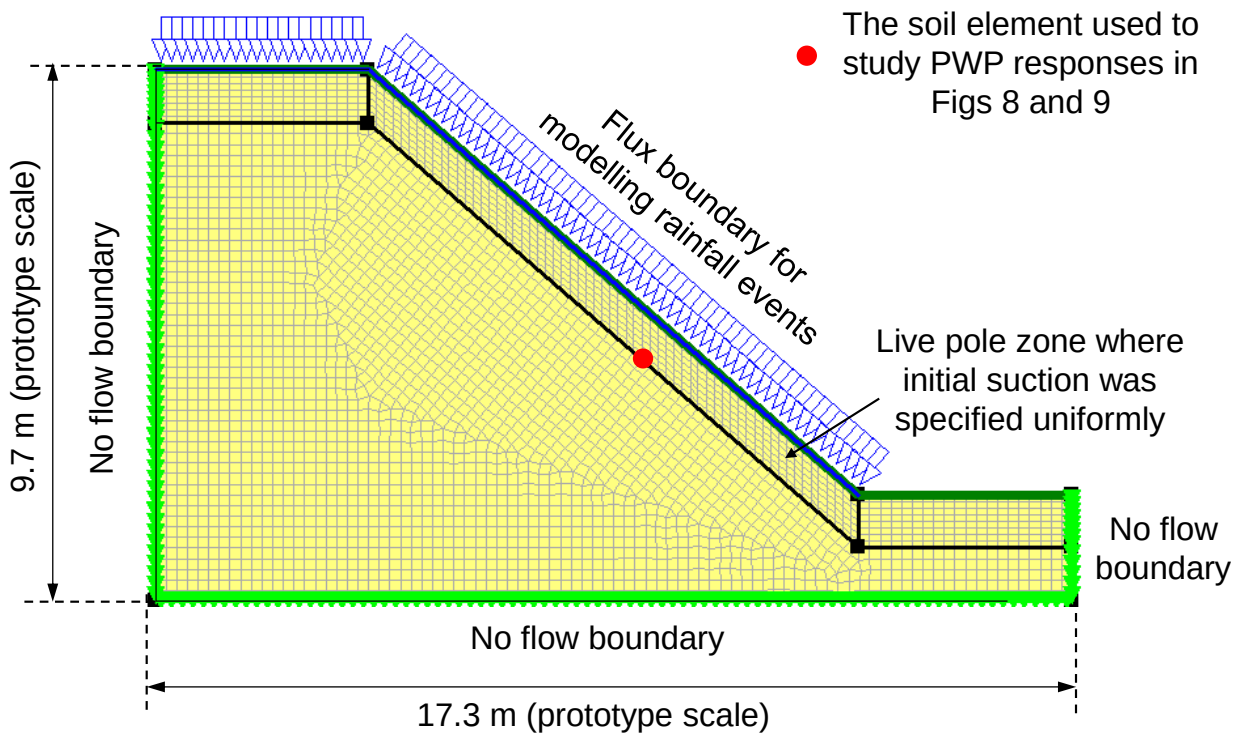

618

619 **Fig. 7** FE mesh and boundary conditions for transient seepage analysis in SEEP/W modelled

620 in prototype scale

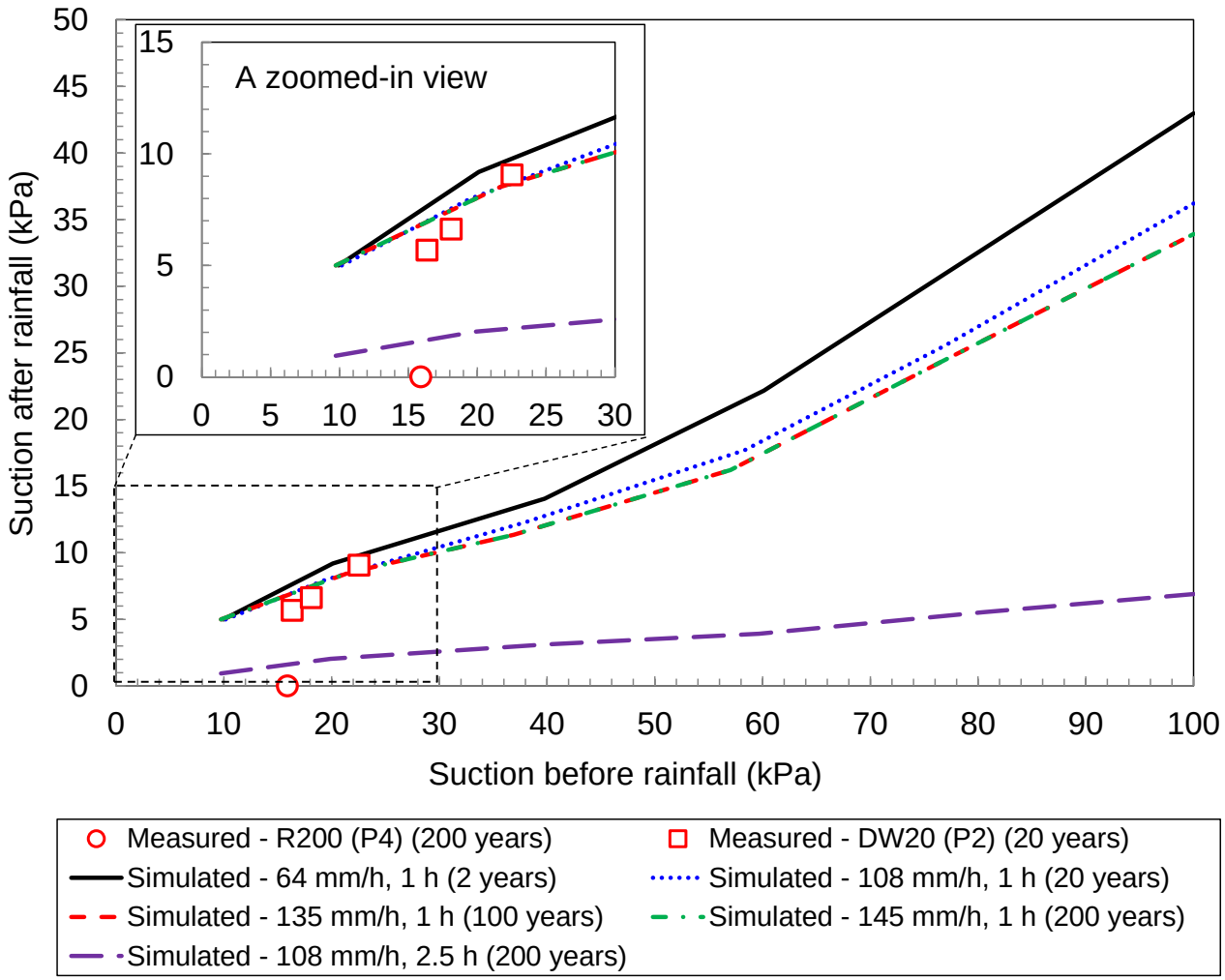

621

622 **Fig. 8** Correlation of suction before and after rainfall

623

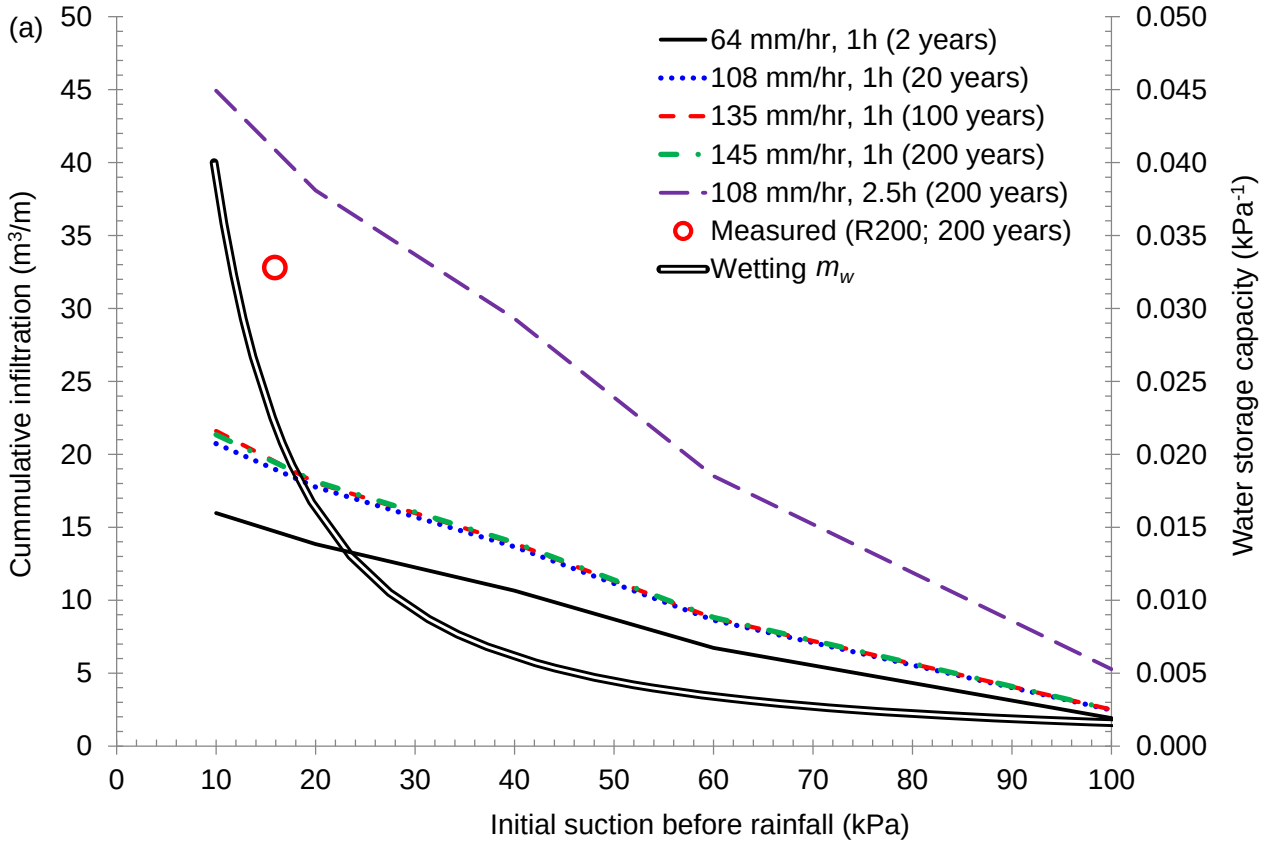

624

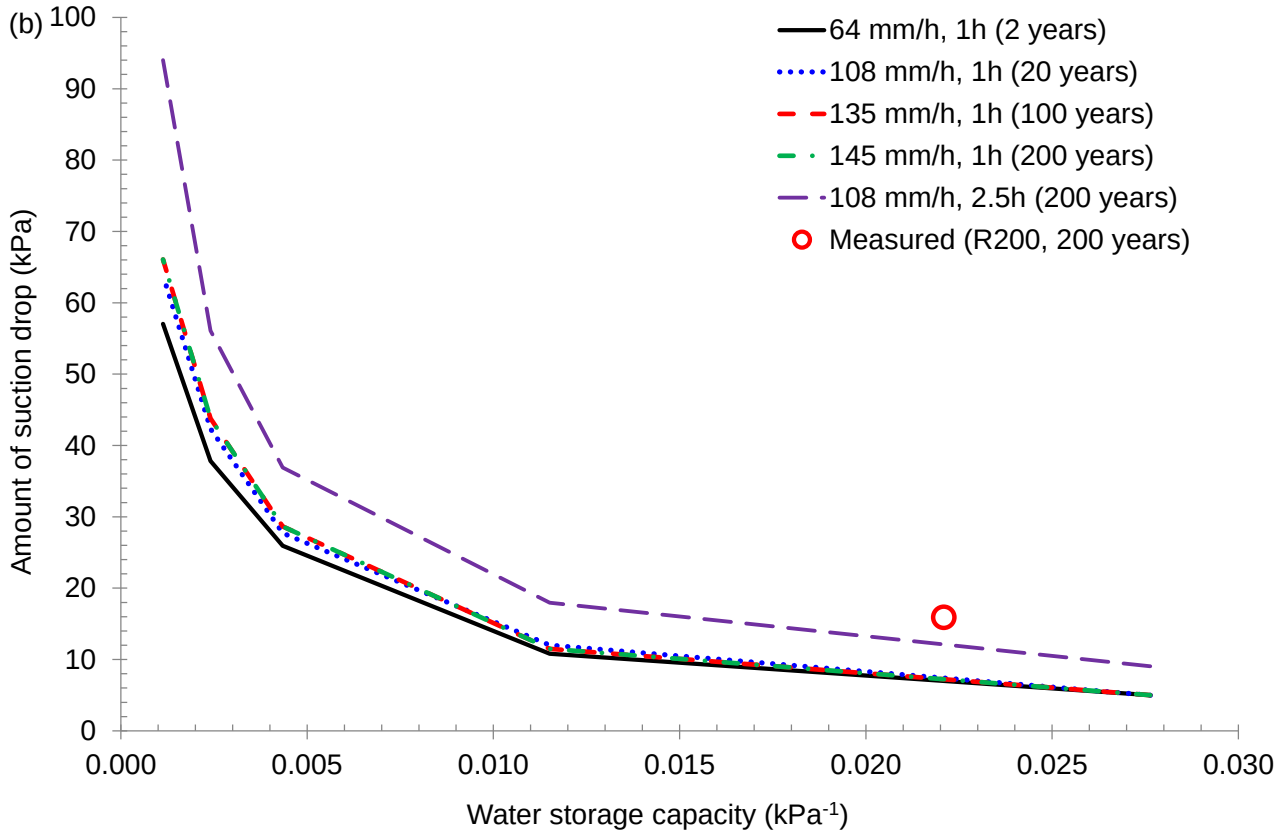

625

626 **Fig. 9** (a) Effects of initial suction on cumulative infiltration and water storage capacity; and
627 (b) effects of water storage capacity on suction drop resulting from infiltration